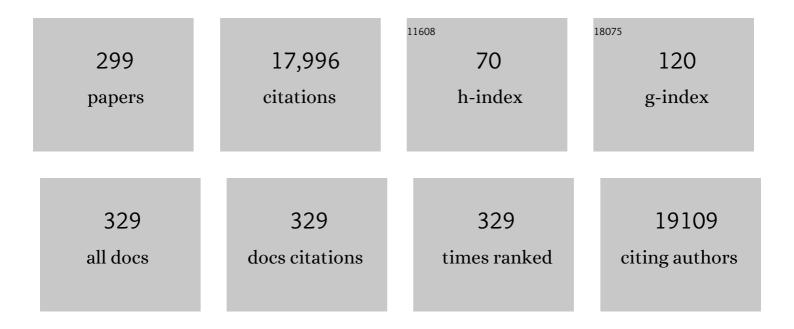
List of Publications by Year in descending order

Source: https://exaly.com/author-pdf/2275927/publications.pdf Version: 2024-02-01



Шигомс 7ноц

#	Article	IF	CITATIONS
1	Trititanate Nanotubes Made via a Single Alkali Treatment. Advanced Materials, 2002, 14, 1208-1211.	11.1	806
2	Metal–Organicâ€Frameworkâ€Đerived Hybrid Carbon Nanocages as a Bifunctional Electrocatalyst for Oxygen Reduction and Evolution. Advanced Materials, 2017, 29, 1700874.	11.1	678
3	Cubic Mesoporous Silica with Large Controllable Entrance Sizes and Advanced Adsorption Properties. Angewandte Chemie - International Edition, 2003, 42, 3146-3150.	7.2	487
4	Alumination and Ion Exchange of Mesoporous SBA-15 Molecular Sieves. Chemistry of Materials, 1999, 11, 1621-1627.	3.2	393
5	Mesopore Molecular Sieve MCM-41 Containing Framework Aluminum. The Journal of Physical Chemistry, 1995, 99, 1018-1024.	2.9	391
6	Disruption of extended defects in solid oxide fuel cell anodes for methane oxidation. Nature, 2006, 439, 568-571.	13.7	379
7	Formation Mechanism ofH2Ti3O7Nanotubes. Physical Review Letters, 2003, 91, 256103.	2.9	331
8	Nanoscale Microelectrochemical Cells on Carbon Nanotubes. Small, 2007, 3, 1513-1517.	5.2	285
9	Low-Temperature Strategy to Synthesize Highly Ordered Mesoporous Silicas with Very Large Pores. Journal of the American Chemical Society, 2005, 127, 10794-10795.	6.6	251
10	Photoluminescence Tuning via Cation Substitution in Oxonitridosilicate Phosphors: DFT Calculations, Different Site Occupations, and Luminescence Mechanisms. Chemistry of Materials, 2014, 26, 2991-3001.	3.2	244
11	A Reliable Synthesis of Cubic Mesoporous MCM-48 Molecular Sieve. Chemistry of Materials, 1998, 10, 3690-3698.	3.2	227
12	Formation Mechanism of Porous Anodic Aluminium and Titanium Oxides. Advanced Materials, 2008, 20, 3663-3667.	11.1	214
13	Formation Mechanism of CaTiO ₃ Hollow Crystals with Different Microstructures. Journal of the American Chemical Society, 2010, 132, 14279-14287.	6.6	198
14	Structural Ordering and Charge Variation Induced by Cation Substitution in (Sr,Ca)AlSiN ₃ :Eu Phosphor. Journal of the American Chemical Society, 2015, 137, 8936-8939.	6.6	198
15	Formation, Structure, and Stability of Titanate Nanotubes and Their Proton Conductivity. Journal of Physical Chemistry B, 2005, 109, 5439-5444.	1.2	194
16	Chemically blockable transformation and ultraselective low-pressure gas adsorption in a non-porous metal organic framework. Nature Chemistry, 2009, 1, 289-294.	6.6	190
17	Enhanced Photoluminescence Emission and Thermal Stability from Introduced Cation Disorder in Phosphors. Journal of the American Chemical Society, 2017, 139, 11766-11770.	6.6	190
18	Formation Mechanism of Porous Single-Crystal Cr2O3and Co3O4Templated by Mesoporous Silica. Chemistry of Materials, 2006, 18, 3088-3095.	3.2	184

#	Article	IF	CITATIONS
19	Self-Construction of Coreâ^'Shell and Hollow Zeolite Analcime Icositetrahedra:  A Reversed Crystal Growth Process via Oriented Aggregation of Nanocrystallites and Recrystallization from Surface to Core. Journal of the American Chemical Society, 2007, 129, 13305-13312.	6.6	175
20	Formation, morphology control and applications of anodic TiO2 nanotube arrays. Journal of Materials Chemistry, 2011, 21, 8955.	6.7	175
21	Synthesis and Characterization of the Mesoporous Silicate Molecular Sieve MCM-48. Journal of Physical Chemistry B, 1997, 101, 5294-5300.	1.2	173
22	Preparation of three-dimensional chromium oxide porous single crystals templated by SBA-15. Chemical Communications, 2003, , 98-99.	2.2	169
23	Unique hole-accepting carbon-dots promoting selective carbon dioxide reduction nearly 100% to methanol by pure water. Nature Communications, 2020, 11, 2531.	5.8	168
24	Polymerized carbon nanobells and their field-emission properties. Applied Physics Letters, 1999, 75, 3105-3107.	1.5	164
25	Site-Directed Surface Derivatization of MCM-41: Use of High-Resolution Transmission Electron Microscopy and Molecular Recognition for Determining the Position of Functionality within Mesoporous Materials. Angewandte Chemie - International Edition, 1998, 37, 2719-2723.	7.2	159
26	Effect of structural aluminium on the mesoporous structure of MCM-41. Journal of the Chemical Society, Faraday Transactions, 1995, 91, 2955.	1.7	146
27	Cell-Targeting Multifunctional Nanospheres with both Fluorescence and Magnetism. Small, 2005, 1, 506-509.	5.2	142
28	Asymmetric Oxygen Vacancies: the Intrinsic Redox Active Sites in Metal Oxide Catalysts. Advanced Science, 2020, 7, 1901970.	5.6	141
29	Bimetallic Nanoparticle Catalysts Anchored Inside Mesoporous Silica. Angewandte Chemie International Edition in English, 1997, 36, 2242-2245.	4.4	139
30	Green Light-Excitable Ce-Doped Nitridomagnesoaluminate Sr[Mg ₂ Al ₂ N ₄] Phosphor for White Light-Emitting Diodes. Chemistry of Materials, 2016, 28, 6822-6825.	3.2	138
31	Direct Preparation of Nanoporous Carbon by Nanocasting. Journal of the American Chemical Society, 2003, 125, 3444-3445.	6.6	137
32	Synthesis and Characterization of the Gallosilicate Mesoporous Molecular Sieve MCM-41. The Journal of Physical Chemistry, 1996, 100, 390-396.	2.9	134
33	Structural Elucidation of Microporous and Mesoporous Catalysts and Molecular Sieves by High-Resolution Electron Microscopy. Accounts of Chemical Research, 2001, 34, 583-594.	7.6	132
34	Recyclable Polyurea-Microencapsulated Pd(0) Nanoparticles:  An Efficient Catalyst for Hydrogenolysis of Epoxides. Organic Letters, 2003, 5, 4665-4668.	2.4	132
35	Growth of porous single-crystal Cr2O3 in a 3-D mesopore system. Chemical Communications, 2005, , 5618.	2.2	131
36	Syntheses, Li Insertion, and Photoactivity of Mesoporous Crystalline TiO ₂ . Advanced Functional Materials, 2009, 19, 2826-2833.	7.8	131

#	Article	IF	CITATIONS
37	Crystal Structure and Growth Mechanism of Unusually Long Fullerene (C ₆₀) Nanowires. Journal of the American Chemical Society, 2008, 130, 2527-2534.	6.6	129
38	Early Stage Reversed Crystal Growth of Zeolite A and Its Phase Transformation to Sodalite. Journal of the American Chemical Society, 2009, 131, 17986-17992.	6.6	129
39	Controllable selective exfoliation of high-quality graphene nanosheets and nanodots by ionic liquid assisted grinding. Chemical Communications, 2012, 48, 1877.	2.2	124
40	A three-dimensional Mn ₃ O ₄ network supported on a nitrogenated graphene electrocatalyst for efficient oxygen reduction reaction in alkaline media. Journal of Materials Chemistry A, 2014, 2, 14493-14501.	5.2	120
41	Zeolite GdNaY Nanoparticles with Very High Relaxivity for Application as Contrast Agents in Magnetic Resonance Imaging. Chemistry - A European Journal, 2002, 8, 5121-5131.	1.7	119
42	Mesoporous Monocrystalline TiO ₂ and Its Solid-State Electrochemical Properties. Chemistry of Materials, 2009, 21, 2540-2546.	3.2	114
43	Crystalline WO3 nanowires synthesized by templating method. Chemical Physics Letters, 2003, 377, 317-321.	1.2	113
44	Controlling the channel diameter of the mesoporous molecular sieve MCM-41. Journal of the Chemical Society, Faraday Transactions, 1997, 93, 359-363.	1.7	112
45	Structural, thermal and electrochemical properties of layered perovskite SmBaCo2O5+d, a potential cathode material for intermediate-temperature solid oxide fuel cells. Journal of Power Sources, 2009, 194, 704-711.	4.0	111
46	Crystalline mesoporous metal oxide. Progress in Natural Science: Materials International, 2008, 18, 1329-1338.	1.8	110
47	Porous crystals of cubic metal oxides templated by cage-containing mesoporous silica. Journal of Materials Chemistry, 2007, 17, 4947.	6.7	105
48	Synthesis and field-emission behavior of highly oriented boron carbonitride nanofibers. Applied Physics Letters, 2000, 76, 2624-2626.	1.5	104
49	Zeolites with Continuously Tuneable Porosity. Angewandte Chemie - International Edition, 2014, 53, 13210-13214.	7.2	104
50	Synthesis and characterization of hybrid organic/inorganic nanotubes of the imogolite type and their behaviour towards methane adsorption. Physical Chemistry Chemical Physics, 2011, 13, 744-750.	1.3	102
51	Investigation of the pore formation in anodic aluminium oxide. Journal of Materials Chemistry, 2008, 18, 5787.	6.7	95
52	Cubic Mesoporous Silica with Large Controllable Entrance Sizes and Advanced Adsorption Properties. Angewandte Chemie, 2003, 115, 3254-3258.	1.6	94
53	Synthesis, Structure Solution, Characterization, and Catalytic Properties of TNU-10:Â A High-Silica Zeolite with the STI Topology. Journal of the American Chemical Society, 2004, 126, 5817-5826.	6.6	93
54	Ternary CdS/Au/3DOM-SrTiO 3 composites with synergistic enhancement for hydrogen production from visible-light photocatalytic water splitting. Applied Catalysis B: Environmental, 2017, 215, 74-84.	10.8	93

#	Article	IF	CITATIONS
55	Control of Luminescence by Tuning of Crystal Symmetry and Local Structure in Mn ⁴⁺ â€Activated Narrow Band Fluoride Phosphors. Angewandte Chemie - International Edition, 2018, 57, 1797-1801.	7.2	93
56	Mesoporous single-crystal Co3O4 templated by cage-containing mesoporous silica. Chemical Communications, 2007, , 2518.	2.2	91
57	Chemical Pressure Control for Photoluminescence of MSiAl ₂ O ₃ N ₂ :Ce ³⁺ /Eu ²⁺ (M = Sr, Ba) Oxynitride Phosphors. Chemistry of Materials, 2014, 26, 2075-2085.	3.2	91
58	Layered Intergrowth Phases Bi4MO8X (X=Cl, M=Ta and X=Br, M=Ta or Nb): Structural and Electrophysical Characterization. Journal of Solid State Chemistry, 2002, 166, 148-157.	1.4	87
59	Synthesis of Periodic Mesoporous Ethylenesilica under Acidic Conditions. Chemistry of Materials, 2004, 16, 1756-1762.	3.2	84
60	New insight into the soot nanoparticles in a candle flame. Chemical Communications, 2011, 47, 4700.	2.2	84
61	Reversed Crystal Growth: Implications for Crystal Engineering. Advanced Materials, 2010, 22, 3086-3092.	11.1	83
62	Facile Surfactantâ€Free Synthesis of pâ€Type SnSe Nanoplates with Exceptional Thermoelectric Power Factors. Angewandte Chemie - International Edition, 2016, 55, 6433-6437.	7.2	81
63	Highly efficient catalysts for the hydrogenation of nitro-substituted aromatics. Chemical Communications, 2005, , 2026.	2.2	76
64	Cubes of Zeoliteâ€A with an Amorphous Core. Angewandte Chemie - International Edition, 2008, 47, 8397-8399.	7.2	76
65	3D to 2D Routes to Ultrathin and Expanded Zeolitic Materials. Chemistry of Materials, 2013, 25, 542-547.	3.2	76
66	One‣tep Synthesis of Bismuth Telluride Nanosheets of a Few Quintuple Layers in Thickness. Angewandte Chemie - International Edition, 2011, 50, 10397-10401.	7.2	75
67	Direct Observation of Growth Defects in Zeolite Beta. Journal of the American Chemical Society, 2005, 127, 494-495.	6.6	74
68	Structural studies on W6+ and Nd3+ substituted La2Mo2O9 materials. Journal of Solid State Chemistry, 2006, 179, 278-288.	1.4	73
69	Crepe Cake Structured Layered Double Hydroxide/Sulfur/Graphene as a Positive Electrode Material for Li–S Batteries. ACS Nano, 2020, 14, 8220-8231.	7.3	73
70	Imaging the Pore Structure and Polytypic Intergrowths in Mesoporous Silica. Journal of Physical Chemistry B, 1998, 102, 6933-6936.	1.2	72
71	Synthesis of Periodic Mesoporous Phenylenesilica under Acidic Conditions with Novel Molecular Order in the Pore Walls. Chemistry of Materials, 2003, 15, 4886-4889.	3.2	72
72	Multiple Nucleation and Crystal Growth of Barium Titanate. Crystal Growth and Design, 2012, 12, 1247-1253.	1.4	71

#	Article	IF	CITATIONS
73	Zeolite Nanocrystals Inside Mesoporous TUD-1: A High-Performance Catalytic Composite. Chemistry - A European Journal, 2004, 10, 4970-4976.	1.7	70
74	Highly active mesostructured silica hosted silver catalysts for CO oxidation using the one-pot synthesis approach. Chemical Communications, 2008, , 2677.	2.2	70
75	Formation, microstructures and crystallization of anodic titanium oxide tubular arrays. Journal of Materials Chemistry, 2009, 19, 2301.	6.7	69
76	Directing the pore dimensions in the mesoporous molecular sieve MCM-41. Chemical Physics Letters, 1996, 263, 247-252.	1.2	67
77	Hierarchical interlinked structure of titanium oxide nanofibers. Chemical Communications, 2002, , 1202-1203.	2.2	67
78	NMR Transversal Relaxivity of Suspensions of Lanthanide Oxide Nanoparticles. Journal of Physical Chemistry C, 2007, 111, 10240-10246.	1.5	67
79	Single-template synthesis of zeolite ZSM-5 composites with tunable mesoporosity. Chemical Communications, 2007, , 4653.	2.2	67
80	Experimental and theoretical investigations of Cs+ adsorption on crown ethers modified magnetic adsorbent. Journal of Hazardous Materials, 2019, 371, 712-720.	6.5	66
81	Synthesis, modification and characterization of K4Nb6O17-type nanotubes. Journal of Materials Chemistry, 2004, 14, 1437.	6.7	65
82	Ru/TiO2-catalysed hydrogenation of xylose: the role of the crystal structure of the support. Catalysis Science and Technology, 2016, 6, 577-582.	2.1	65
83	Chlorineâ€Enabled Electron Doping in Solutionâ€5ynthesized SnSe Thermoelectric Nanomaterials. Advanced Energy Materials, 2017, 7, 1602328.	10.2	64
84	Wheat Germ Agglutinin-Modified Trifunctional Nanospheres for Cell Recognition. Bioconjugate Chemistry, 2007, 18, 1749-1755.	1.8	62
85	The `silica garden': a hierarcharical nanostructure. Chemical Physics Letters, 1998, 286, 88-92.	1.2	61
86	The Ti ₃ AlC ₂ MAX Phase as an Efficient Catalyst for Oxidative Dehydrogenation of nâ€Butane. Angewandte Chemie - International Edition, 2018, 57, 1485-1490.	7.2	61
87	Defect fluorite-related superstructures in the Bi2O3î—,V2O5 system. Journal of Solid State Chemistry, 1988, 76, 290-300.	1.4	60
88	Synthesis and structural studies of the perovskite-related compound YBaCo2O5 + x. Advanced Materials, 1993, 5, 735-738.	11.1	60
89	Ferroelectric Properties and Crystal Structure of the Layered Intergrowth Phase Bi3Pb2Nb2O11Cl. Chemistry of Materials, 2001, 13, 4731-4737.	3.2	60
90	Dissociation of Water During Formation of Anodic Aluminum Oxide. Journal of the American Chemical Society, 2009, 131, 8697-8702.	6.6	60

#	Article	IF	CITATIONS
91	Preparation and characterization of three-dimensional mesoporous crystals of tungsten oxide. Chemical Physics Letters, 2005, 407, 83-86.	1.2	59
92	The role of Bi-doping in promoting electron transfer and catalytic performance of Pt/3DOM-Ce1â^'Bi O2â^'δ. Journal of Catalysis, 2018, 365, 292-302.	3.1	59
93	Highâ€resolution imaging of nanoparticle bimetallic catalysts supported on mesoporous silica. Catalysis Letters, 1999, 60, 113-120.	1.4	58
94	Title is missing!. Catalysis Letters, 2001, 72, 203-206.	1.4	57
95	Blue Emission by Interstitial Site Occupation of Ce ³⁺ in AlN. Chemistry of Materials, 2012, 24, 3486-3492.	3.2	57
96	Anodic formation of nanoporous and nanotubular metal oxides. Journal of Materials Chemistry, 2012, 22, 535-544.	6.7	57
97	Controlling of Structural Ordering and Rigidity of Î ² -SiAlON:Eu through Chemical Cosubstitution to Approach Narrow-Band-Emission for Light-Emitting Diodes Application. Chemistry of Materials, 2017, 29, 6781-6792.	3.2	57
98	A Highly Efficient Coordination Polymer for Selective Trapping and Sensing of Perrhenate/Pertechnetate. ACS Applied Materials & Interfaces, 2020, 12, 15246-15254.	4.0	57
99	Temperature-Dependent Raman Scattering of Silicon Nanowires. Journal of Physical Chemistry B, 2006, 110, 1229-1234.	1.2	55
100	Co/carbon-nanotube monometallic system: the effects of oxidation by nitric acid. Physical Chemistry Chemical Physics, 2001, 3, 2518-2521.	1.3	54
101	Facile synthesis of ZSM-5 composites with hierarchical porosity. Journal of Materials Chemistry, 2008, 18, 468-474.	6.7	54
102	Robust Antiferromagnetism and Structural Disorder in BixCa1â^'xFeO3 Perovskites. Chemistry of Materials, 2009, 21, 2085-2093.	3.2	54
103	Superlattices in ternary oxides derived from bismuth oxide (Bi2O3): new families of ordered phases based on the fluorite structure. The Journal of Physical Chemistry, 1987, 91, 512-514.	2.9	53
104	What Can Electron Microscopy Tell Us Beyond Crystal Structures?. European Journal of Inorganic Chemistry, 2016, 2016, 941-950.	1.0	53
105	Active Oxygen Species Promoted Catalytic Oxidation of 5-Hydroxymethyl-2-furfural on Facet-Specific Pt Nanocrystals. ACS Catalysis, 2019, 9, 8306-8315.	5.5	53
106	Structural chemistry and physical properties of some ternary oxides in the Bi2O3Ta2O5 system. Journal of Solid State Chemistry, 1992, 101, 1-17.	1.4	52
107	Defect Fluorite Superstructures in the Bi2O3-WO3 System. Journal of Solid State Chemistry, 1994, 108, 381-394.	1.4	51
108	A novel ordered cubic mesoporous silica templated with tri-head group quaternary ammonium surfactantElectronic supplementary information (ESI) available: projections of a typical diamond structure with Fd3m space group; 1H NMR data; elemental analysis; SEM image; experimental characterization. See http://www.rsc.org/suppdata/cc/b2/b206993h/. Chemical Communications, 2002, , 2212-2213.	2.2	50

#	Article	IF	CITATIONS
109	The mechanism of channel formation in the mesoporous molecular sieve MCM-41. Chemical Physics Letters, 1998, 292, 207-212.	1.2	49
110	Aluminate Red Phosphor in Light-Emitting Diodes: Theoretical Calculations, Charge Varieties, and High-Pressure Luminescence Analysis. ACS Applied Materials & Interfaces, 2017, 9, 23995-24004.	4.0	49
111	Transformation of lamellar silicate into the mesoporous molecular sieve MCM-41. Journal of the Chemical Society, Faraday Transactions, 1998, 94, 979-983.	1.7	48
112	Structural Chemistry and Conductivity of a Solid Solution of YBa ₁₋ <i>_x</i> Sr <i>_x</i> Co ₂ O ₅₊ _{î´} . Journal of Physical Chemistry C, 2007, 111, 19120-19125.	1.5	47
113	Microstructural study of the formation mechanism of metal–organic framework MOF-5. CrystEngComm, 2014, 16, 1064-1070.	1.3	47
114	A simple method for coating carbon nanotubes with Co–B amorphous alloy. Materials Letters, 2003, 57, 1339-1344.	1.3	46
115	Synthesis and Formation Mechanism of Textured MOF-5. Crystal Growth and Design, 2016, 16, 2104-2111.	1.4	46
116	Title is missing!. Catalysis Letters, 2002, 82, 95-98.	1.4	45
117	TUD-C: A tunable, hierarchically structured mesoporous zeolite composite. Microporous and Mesoporous Materials, 2009, 120, 19-28.	2.2	45
118	M ³⁺ O(–Mn ⁴⁺) ₂ clusters in doped MnO _x catalysts as promoted active sites for the aerobic oxidation of 5-hydroxymethylfurfural. Catalysis Science and Technology, 2018, 8, 2299-2303.	2.1	45
119	Nanosegregation and Neighbor ation Control of Photoluminescence in Carbidonitridosilicate Phosphors. Angewandte Chemie - International Edition, 2013, 52, 8102-8106.	7.2	44
120	One-step synthesis and shape-control of CuPd nanowire networks. Nanoscale, 2014, 6, 1093-1098.	2.8	44
121	Membrane lipid peroxidation by the peroxidase-like activity of magnetite nanoparticles. Chemical Communications, 2014, 50, 11147-11150.	2.2	44
122	A novel morphology of mesoporous molecular sieve MCM-41. Chemical Physics Letters, 2001, 333, 427-431.	1.2	43
123	Gadolinium(III)-Loaded Nanoparticulate Zeolites as Potential High-Field MRI Contrast Agents: Relationship Between Structure and Relaxivity. Chemistry - A European Journal, 2005, 11, 4799-4807.	1.7	42
124	Synthesis, structure and thermal transformations of aluminophosphates containing the nickel complex [Ni(diethylenetriamine)2]2+ as a structure directing agent. Microporous and Mesoporous Materials, 2003, 58, 91-104.	2.2	41
125	Controlled Synthesis, Characterization, and Crystallization of Niâ [~] 'P Nanospheres. Journal of Physical Chemistry B, 2005, 109, 24361-24368.	1.2	41
126	Crystallographic and magnetic studies of mesoporous eskolaite,. Microporous and Mesoporous Materials, 2010, 130, 280-286.	2.2	41

#	Article	IF	CITATIONS
127	Ultra-small photoluminescent silicon-carbide nanocrystals by atmospheric-pressure plasmas. Nanoscale, 2016, 8, 17141-17149.	2.8	41
128	Crystal morphology supports the liquid crystal formation mechanism for the mesoporous molecular sieve MCM-41. Chemical Physics Letters, 1995, 244, 117-120.	1.2	40
129	Pore diameter control in anodic titanium and aluminium oxides. Journal of Materials Chemistry, 2011, 21, 357-362.	6.7	40
130	Relaxor-to-Ferroelectric Crossover and Disruption of Polar Order in "Empty―Tetragonal Tungsten Bronzes. Chemistry of Materials, 2016, 28, 4616-4627.	3.2	40
131	A new family of photocatalysts based on Bi2O3. Journal of Solid State Chemistry, 1988, 72, 126-130.	1.4	39
132	A method for the synthesis of high quality large crystal MCM-41. Chemical Communications, 1999, , 51-52.	2.2	39
133	Electron diffraction and HRTEM imaging of beam-sensitive materials. Crystallography Reviews, 2011, 17, 163-185.	0.4	39
134	Solid Solution of YBaCuxCo2-xO5 (0 .ltoreq. x .ltoreq. 1) and Its Intergrowth with YBa2Cu3O7. Chemistry of Materials, 1994, 6, 441-447.	3.2	38
135	TNU-7:  A Large-Pore Gallosilicate Zeolite Constructed of Strictly Alternating MOR and MAZ Layers. Chemistry of Materials, 2005, 17, 1272-1274.	3.2	38
136	A new anode for solid oxide fuel cells with enhanced OCV under methane operation. Physical Chemistry Chemical Physics, 2007, 9, 1821-1830.	1.3	38
137	Electron-beam induced formation of nanoparticle chains and wires from a ruthenium cluster polymer. Chemical Communications, 2000, , 1317-1318.	2.2	37
138	Restructuring of mesoporous silica: high quality large crystal MCMâ€41 via a seeded recrystallisation route. Journal of Materials Chemistry, 2000, 10, 1139-1145.	6.7	37
139	Hierarchical structured graphene/metal oxide/porous carbon composites as anode materials for lithium-ion batteries. Materials Research Bulletin, 2016, 73, 102-110.	2.7	37
140	STA-20: An ABC-6 Zeotype Structure Prepared by Co-Templating and Solved via a Hypothetical Structure Database and STEM-ADF Imaging. Chemistry of Materials, 2017, 29, 2180-2190.	3.2	37
141	Title is missing!. Catalysis Letters, 2002, 84, 1-5.	1.4	36
142	Sc-Substituted Oxygen Excess Titanates as Fuel Electrodes for SOFCs. Journal of the Electrochemical Society, 2005, 152, A1458.	1.3	36
143	A systematic study of the formation of mesostructured silica using surfactant ruthenium complexes in high- and low-concentration regimes. Journal of Materials Chemistry, 2008, 18, 5282.	6.7	36
144	Assessing Molecular Transport Properties of Nanoporous Materials by Interference Microscopy: Remarkable Effects of Composition and Microstructure on Diffusion in the Silicoaluminophosphate Zeotype STA-7. Journal of the American Chemical Society, 2010, 132, 11665-11670.	6.6	36

#	Article	IF	CITATIONS
145	In situ EPR studies of electron trapping in a nanocrystalline rutile. Journal of Photochemistry and Photobiology A: Chemistry, 2010, 216, 238-243.	2.0	35
146	Novel Large-Pore Aluminophosphate Molecular Sieve STA-15 Prepared Using the Tetrapropylammonium Cation As a Structure Directing Agent. Chemistry of Materials, 2010, 22, 338-346.	3.2	35
147	Improved Optoelectronic Properties of Silicon Nanocrystals/Polymer Nanocomposites by Microplasma-Induced Liquid Chemistry. Journal of Physical Chemistry C, 2013, 117, 23198-23207.	1.5	35
148	The type II superstructural family in the Bi2O3î—,V2O5 system. Journal of Solid State Chemistry, 1990, 87, 44-54.	1.4	34
149	Synthesis and Characterization of Gibbsite Nanostructures. Journal of Physical Chemistry C, 2008, 112, 4124-4128.	1.5	33
150	The application of inelastic neutron scattering to investigate CO hydrogenation over an iron Fischer–Tropsch synthesis catalyst. Journal of Catalysis, 2014, 312, 221-231.	3.1	33
151	Dipole Field Guided Orientated Attachment of Nanocrystals to Twinâ€Brush ZnO Mesocrystals. Chemistry - A European Journal, 2012, 18, 16104-16113.	1.7	32
152	Directly Imaging Interstitial Oxygen in Silicate Apatite. Advanced Energy Materials, 2012, 2, 316-321.	10.2	32
153	Ultrafast Elemental and Oxidation-State Mapping of Hematite by 4D Electron Microscopy. Journal of the American Chemical Society, 2017, 139, 4916-4922.	6.6	32
154	Aptamer conjugated Mo6S9â^'l nanowires for direct and highly sensitive electrochemical sensing of thrombin. Biosensors and Bioelectronics, 2011, 26, 1853-1859.	5.3	31
155	The origin of ZnO twin crystals in bio-inspired synthesis. CrystEngComm, 2012, 14, 1247-1255.	1.3	31
156	Synthesis, characterization and control of faulting in STF/SFF topologies, a new family of intergrowth zeolitesElectronic supplementary information (ESI) available: details of DIFFaX simulations. See http://www.rsc.org/suppdata/jm/b3/b315643e/. Journal of Materials Chemistry, 2004, 14, 1982.	6.7	30
157	Preparation of α-Fe ₂ O ₃ hollow spheres, nanotubes, nanoplates and nanorings as highly efficient Cr(<scp>vi</scp>) adsorbents. RSC Advances, 2016, 6, 82854-82861.	1.7	30
158	Efficient Luminescence from CsPbBr ₃ Nanoparticles Embedded in Cs ₄ PbBr ₆ . Journal of Physical Chemistry Letters, 2020, 11, 7637-7642.	2.1	29
159	Nanoscale Super Clusters of Clusters Assembled around a Dendritic Core. Angewandte Chemie - International Edition, 2000, 39, 1661-1664.	7.2	28
160	Uncovering a Solvent-Controlled Preferential Growth of Buckminsterfullerene (C ₆₀) Nanowires. Journal of Physical Chemistry C, 2009, 113, 6390-6397.	1.5	28
161	Crystal growth of Si nanowires and formation of longitudinal planar defects. CrystEngComm, 2010, 12, 2793.	1.3	28
162	Facile Synthesis of Branched Ruthenium Nanocrystals and Their Use in Catalysis. Crystal Growth and Design, 2012, 12, 939-942.	1.4	28

#	Article	IF	CITATIONS
163	Topotactic anion-exchange in thermoelectric nanostructured layered tin chalcogenides with reduced selenium content. Chemical Science, 2018, 9, 3828-3836.	3.7	28
164	Particle morphology and microstructure in the mesoporous silicate SBA-2. Journal of Materials Chemistry, 2002, 12, 20-23.	6.7	27
165	Formation Mechanism of Mg2SiO4 Fishbone-like Fractal Nanostructures. Journal of Physical Chemistry B, 2004, 108, 11561-11566.	1.2	27
166	Large-Scale Surfactant-Free Synthesis of p-Type SnTe Nanoparticles for Thermoelectric Applications. Materials, 2017, 10, 233.	1.3	27
167	Rapid synthesis of BiOBrxl1-x photocatalysts: Insights to the visible-light photocatalytic activity and strong deviation from Vegard's law. Catalysis Today, 2019, 335, 477-484.	2.2	27
168	Zeolite-derived hybrid materials with adjustable organic pillars. Chemical Science, 2016, 7, 3589-3601.	3.7	26
169	A unique structure of Cu2(OH)3·NH3 crystals in the `silica garden' and their degradation under electron beam irradiation. Chemical Physics Letters, 1999, 306, 145-148.	1.2	25
170	Synthesis and Structure of Bimetallic Nickel Molybdenum Phosphide Solid Solutions. Chemistry of Materials, 2004, 16, 2697-2699.	3.2	25
171	The Ti ₃ AlC ₂ MAX Phase as an Efficient Catalyst for Oxidative Dehydrogenation of nâ€Butane. Angewandte Chemie, 2018, 130, 1501-1506.	1.6	25
172	Effect of the oxygen coordination environment of Ca–Mn oxides on the catalytic performance of Pd supported catalysts for aerobic oxidation of 5-hydroxymethyl-2-furfural. Catalysis Science and Technology, 2019, 9, 6659-6668.	2.1	25
173	HRTEM surface profile imaging of solids. Current Opinion in Solid State and Materials Science, 2001, 5, 75-83.	5.6	24
174	Mechanism–Property Correlation in Coordination Polymer Crystals toward Design of a Superior Sorbent. ACS Applied Materials & Interfaces, 2019, 11, 42375-42384.	4.0	24
175	Imaging helical potassium hexaniobate nanotubes. Applied Physics Letters, 2003, 83, 1638-1640.	1.5	23
176	Reversed crystal growth of rhombohedral calcite in the presence of chitosan and gum arabic. CrystEngComm, 2013, 15, 10266.	1.3	23
177	Domination of Second-Sphere Shrinkage Effect To Improve Photoluminescence of Red Nitride Phosphors. Inorganic Chemistry, 2014, 53, 12822-12831.	1.9	23
178	The preparation by true liquid crystal templating of mesoporous silicates containing nanoparticulate metals. Chemical Communications, 2006, , 3411.	2.2	22
179	The synthesis of mesoporous silicates containing bimetallic nanoparticles and magnetic properties of PtCo nanoparticles in silica. Chemical Communications, 2006, , 3414.	2.2	22
180	Reversed crystal growth of ZnO microdisks. Chemical Communications, 2013, 49, 5411.	2.2	22

#	Article	IF	CITATIONS
181	MCMâ€41 mit nanometergroßen AgRuâ€Partikeln in den Hohlrämen ―Herstellung, Charakterisierung und Katalysatoreigenschaften. Angewandte Chemie, 1997, 109, 2337-2341.	1.6	21
182	An ordered array of cadmium clusters assembled in zeolite A. Chemical Communications, 2004, , 736.	2.2	21
183	Study on the interaction between tetracene and Cu(110) surface. Journal of Chemical Physics, 2007, 127, 224709.	1.2	21
184	Electronic structures of CuPc on a Ag(110) surface. Journal of Physics Condensed Matter, 2007, 19, 136002.	0.7	21
185	The influence of hydroxide on the initial stages of anodic growth of TiO ₂ nanotubular arrays. Nanotechnology, 2010, 21, 505601.	1.3	21
186	A New Family of Twoâ€Ðimensional Zeolites Prepared from the Intermediate Layered Precursor IPCâ€3P Obtained during the Synthesis of TUN Zeolite. Chemistry - A European Journal, 2013, 19, 13937-13945.	1.7	21
187	Covalently Immobilized Lipase on a Thermoresponsive Polymer with an Upper Critical Solution Temperature as an Efficient and Recyclable Asymmetric Catalyst in Aqueous Media. ChemCatChem, 2018, 10, 1166-1172.	1.8	21
188	Nanoparticles from the decomposition of the complex [InN3(CH2CH2CH2NMe2)2]. Journal of Materials Chemistry, 2004, 14, 3124.	6.7	20
189	Synthesis and characterization of crystalline microporous cobalt phosphite nanowires. Applied Physics Letters, 2005, 87, 173122.	1.5	20
190	The oxidation of water by cerium(iv) catalysed by nanoparticulate RuO2 on mesoporous silica. Dalton Transactions, 2005, , 1027.	1.6	20
191	Neutron powder diffraction and magnetic studies of mesoporous Co3O4. Journal of Magnetism and Magnetic Materials, 2011, 323, 226-231.	1.0	20
192	Formation Mechanism of CaCO3 Spherulites in the Myostracum Layer of Limpet Shells. Crystals, 2017, 7, 319.	1.0	20
193	Cobalt Diselenide Nanorods Grafted on Graphitic Carbon Nitride: A Synergistic Catalyst for Oxygen Reactions in Rechargeable Liâ^'O ₂ Batteries. ChemElectroChem, 2018, 5, 29-35.	1.7	20
194	Porous crystalline iron oxide thin films templated by mesoporous silica. Microporous and Mesoporous Materials, 2005, 83, 219-224.	2.2	19
195	Microscopic study of crystal defects enriches our knowledge of materials chemistry. Journal of Materials Chemistry, 2008, 18, 5321.	6.7	19
196	Semiconducting quantum confined silicon–tin alloyed nanocrystals prepared by ns pulsed laser ablation in water. Nanoscale, 2013, 5, 6725.	2.8	19
197	Iron ochre–Âa preâ€catalyst for the cracking of methane. Journal of Chemical Technology and Biotechnology, 2014, 89, 1317-1323.	1.6	19
198	Multivalent Cation Cross-Linking Suppresses Highly Energetic Graphene Oxide's Flammability. Journal of Physical Chemistry C, 2017, 121, 5829-5835.	1.5	19

#	Article	IF	CITATIONS
199	True liquid crystal templating of SBA-15 with reduced microporosity. Microporous and Mesoporous Materials, 2013, 172, 112-117.	2.2	18
200	"lsofacet―Anatase TiO ₂ Microcages: Topotactic Synthesis and Ultrastable Liâ€Ion Storage. Advanced Materials Interfaces, 2015, 2, 1500210.	1.9	18
201	Electron beam irradiation effect on nanostructured molecular sieve catalysts. Journal of Electron Spectroscopy and Related Phenomena, 2003, 129, 189-194.	0.8	17
202	Alloying and dealloying of CuPt bimetallic nanocrystals. Progress in Natural Science: Materials International, 2013, 23, 331-337.	1.8	17
203	Phase transformation of Mg-calcite to aragonite in active-forming hot spring travertines. Mineralogy and Petrology, 2015, 109, 453-462.	0.4	17
204	Nanocone Decorated ZnO Microspheres Exposing the (0001) Plane and Enhanced Photocatalytic Properties. Advanced Materials Interfaces, 2017, 4, 1601238.	1.9	17
205	Mesoporous VOx–SbOx/SBA-15 synthesized by a two-stage grafting method and its characterization. Chemical Communications, 2001, , 2552-2553.	2.2	16
206	Production of Ultrafine Single-Crystal Copper Wires through Electron Beam Irradiation of Cu-containing Zeolite X. Zeitschrift Fur Anorganische Und Allgemeine Chemie, 2005, 631, 443-447.	0.6	16
207	Dipole field driven morphology evolution in biomimetic vaterite. CrystEngComm, 2016, 18, 1585-1599.	1.3	16
208	Synthesis and characterization of manganese-modified MCM-41. Materials Chemistry and Physics, 2003, 77, 299-303.	2.0	15
209	Advances in Carbonâ€Incorporated Nonâ€Noble Transition Metal Catalysts for Oxygen Reduction Reaction in Polymer Electrolyte Fuel Cells. Journal of the Chinese Chemical Society, 2014, 61, 93-100.	0.8	15
210	Reversed Crystal Growth of RHO Zeolitic Imidazolate Framework (ZIF). Chemistry - A European Journal, 2015, 21, 19090-19095.	1.7	15
211	Growth Mechanism of Dendritic Hematite via Hydrolysis of Ferricyanide. Crystal Growth and Design, 2017, 17, 800-808.	1.4	15
212	Reversed Crystal Growth. Crystals, 2019, 9, 7.	1.0	15
213	Surface trace doping of Na enhancing structure stability and adsorption properties of Li1.6Mn1.6O4 for Li+ recovery. Separation and Purification Technology, 2021, 256, 117583.	3.9	15
214	Atomic Resolution of Oxygen in Solid Oxides by Electron Microscopy: What Next?. ChemPhysChem, 2003, 4, 927-929.	1.0	14
215	Formation mechanism of hollow microspheres consisting of ZnO nanosheets. CrystEngComm, 2012, 14, 8615.	1.3	14
216	The application of inelastic neutron scattering to investigate a hydrogen pre-treatment stage of an iron Fischer–Tropsch catalyst. Applied Catalysis A: General, 2015, 489, 209-217.	2.2	14

#	Article	IF	CITATIONS
217	Structure and cleavage of monosodium urate monohydrate crystals. Chemical Communications, 2019, 55, 2178-2181.	2.2	14
218	Toward New Thermoelectrics: Tin Selenide/Modified Graphene Oxide Nanocomposites. ACS Omega, 2019, 4, 6010-6019.	1.6	13
219	Growth and growth mechanism of oxide nanocrystals on electrochemically exfoliated graphene for lithium storage. Energy Storage Materials, 2019, 18, 174-181.	9.5	13
220	Direct growth of SnO2 nanocrystallites on electrochemically exfoliated graphene for lithium storage. Journal of Energy Storage, 2019, 21, 647-656.	3.9	13
221	Microdomain texture and microstructures of Fe4+-containing CaTi0.4Fe0.6O3â~î´. Journal of Solid State Chemistry, 2004, 177, 3105-3113.	1.4	12
222	A reinvestigation of Sillén X1-type lead tellurium oxyhalides, Pb3TeO4X2 (X = Cl, Br, I). Solid State Sciences, 2006, 8, 1029-1034.	1.5	12
223	Accelerated electron beam induced breakdown of commercial WO3 into nanorods in the presence of triethylamine. Physical Chemistry Chemical Physics, 2011, 13, 20923.	1.3	12
224	Early stages of non-classic crystal growth. Science China Chemistry, 2011, 54, 1867-1876.	4.2	12
225	Formation of anodic TiO2 nanotube arrays with bimodal pore size distribution. Electrochemistry Communications, 2013, 31, 67-70.	2.3	12
226	Highly efficient synthesis of LTA-type aluminophosphate molecular sieve by improved ionothermal method. New Journal of Chemistry, 2016, 40, 2444-2450.	1.4	12
227	Morphogenesis of surface patterns and incorporation of redox-active metals in mesoporous silicate molecular sieves. Surface and Interface Analysis, 2001, 32, 193-197.	0.8	11
228	Microstructures of Some Bi–W–Nb–O Phases. Journal of Solid State Chemistry, 2002, 163, 479-483.	1.4	11
229	Synthesis and characterization of n=5, 6 members of the La4Srnâ~'4TinO3n+2 series with layered structure based upon perovskite. Journal of Solid State Chemistry, 2004, 177, 2039-2043.	1.4	11
230	Syntheses and proton conductivity of mesoporous Nd2O3–SiO2 and NdOCl–SiO2 composites. Journal of Materials Science, 2012, 47, 2146-2154.	1.7	11
231	The role of surface hydrolysis of ferricyanide anions in crystal growth of snowflake-shaped α-Fe ₂ O ₃ . Chemical Communications, 2015, 51, 9350-9353.	2.2	11
232	Aurivillius phases: Non-superconducting materials?. Advanced Materials, 1990, 2, 94-97.	11.1	10
233	HRTEM Surface Profile Imaging of Superconducting YBa2Cu4O8. Journal of Solid State Chemistry, 2000, 149, 327-332.	1.4	10
234	Chemistry of Hydrolysis of FeCl3 in the Presence of Phosphate to Form Hematite Nanotubes and Nanorings. Crystal Growth and Design, 2017, 17, 5975-5983.	1.4	10

#	Article	IF	CITATIONS
235	Phase identification in the Tl2O3î—,BaO system: Ba2Tl2O5 and Ba4Tl6O13. Journal of Solid State Chemistry, 1990, 87, 472-478.	1.4	9
236	Atomic imaging of clear surface of superconducting YBa2Cu3O7-δ. Journal of Solid State Chemistry, 1992, 98, 437-441.	1.4	9
237	Coverage dependence of the structure of tetracene on Ag(110). Journal of Physics Condensed Matter, 2008, 20, 315010.	0.7	9
238	Ionic nano-convection in anodisation of aluminium plate. Chemical Communications, 2009, , 5639.	2.2	9
239	Growth mechanism of C60/mesitylene nanowires. CrystEngComm, 2012, 14, 1449-1454.	1.3	9
240	Surface ligand mediated growth of CuPt nanorods. CrystEngComm, 2014, 16, 1714.	1.3	9
241	Cs7Sm11[TeO3]12Cl16 and Rb7Nd11[TeO3]12Br16, the new tellurite halides of the tetragonal Rb6LiNd11[SeO3]12Cl16 structure type. Journal of Solid State Chemistry, 2015, 232, 56-61.	1.4	9
242	Facile Surfactantâ€Free Synthesis of pâ€Type SnSe Nanoplates with Exceptional Thermoelectric Power Factors. Angewandte Chemie, 2016, 128, 6543-6547.	1.6	9
243	Reversed Crystal Growth of Calcite in Naturally Occurring Travertine Crust. Crystals, 2017, 7, 36.	1.0	9
244	Control of Luminescence by Tuning of Crystal Symmetry and Local Structure in Mn ⁴⁺ â€Activated Narrow Band Fluoride Phosphors. Angewandte Chemie, 2018, 130, 1815-1819.	1.6	9
245	Combined positron-annihilation and structural studies of hydrothermally grown zirconia. Nanomaterials and Energy, 2012, 1, 97-105.	0.1	8
246	Surface Charge Driven Growth of Eight-Branched Cu ₂ O Crystals. Crystal Growth and Design, 2016, 16, 5377-5384.	1.4	8
247	Transmission electron microscopy analysis of some transition metal compounds for energy storage and conversion. TrAC - Trends in Analytical Chemistry, 2017, 90, 62-79.	5.8	8
248	Formation and Near-Infrared Emission of CsPbI ₃ Nanoparticles Embedded in Cs ₄ PbI ₆ Crystals. ACS Applied Materials & Interfaces, 2021, 13, 34742-34751.	4.0	8
249	Vertical graphene nanoflakes for the immobilization, electrocatalytic oxidation and quantitative detection of DNA. Electrochemistry Communications, 2012, 25, 140-143.	2.3	7
250	New mechanism for the nucleation and growth of large zeolite X crystals in the presence of triethanolamine. Chemical Communications, 2019, 55, 862-865.	2.2	7
251	Formation Mechanisms of ZnO Spherulites and Derivatives. Crystal Growth and Design, 2019, 19, 249-257.	1.4	7
252	Characterisation of novel anodes for solid oxide fuel cells based on oxygen-excess perovskite related structures. Ionics, 2002, 8, 252-255.	1.2	6

#	Article	IF	CITATIONS
253	Transition metal ion-induced morphogenesis of mesoporous molecular sieve MCM-41. Chemical Physics Letters, 2002, 361, 307-311.	1.2	6
254	The adsorption with chiral structure of fluorene-1-carboxylic acid molecules on Cu(110) surface. Chemical Physics Letters, 2008, 452, 275-280.	1.2	6
255	Synthesis and in situ transformation of PST-1: a potassium gallosilicate natrolite with a high Ga content. Dalton Transactions, 2010, 39, 2246.	1.6	6
256	Intermediate compositions in the series BI ₂ O ₃₋ M ₂ O ₅ structures incorporating elements of pervoskite and fluorite. Geophysical Monograph Series, 0, , 113-117.	0.1	6
257	Formation, crystal growth and colour appearance of Mimetic Tianmu glaze. Ceramics International, 2016, 42, 7506-7513.	2.3	6
258	An efficient synthetic strategy for uniform perovskite core–shell nanocubes NaMgF ₃ :Mn ²⁺ ,Yb ³⁺ @NaMgF ₃ :Yb ³⁺ enhanced near infrared upconversion luminescence. Journal of Materials Chemistry C, 2018, 6, 2342-2350.	2.7	6
259	Superstructures and band gaps of bismuth tantalum oxide solid solutions. Advanced Materials, 1990, 2, 414-420.	11.1	5
260	Two perovskite-related materials for future superconductivity. Physica C: Superconductivity and Its Applications, 1991, 190, 59-61.	0.6	5
261	A study of the upper limit of borate substitution in LnSr2Cu3â^'xBxO7 materials. Journal of Alloys and Compounds, 1997, 261, 187-191.	2.8	5
262	Synthesis of Microporous Silica in the Presence of Dodecyldimethylbenzylammonium Chloride Surfactant. Chemistry Letters, 2000, 29, 1150-1151.	0.7	5
263	HRTEM of negative replicas of mesoporous silica. Studies in Surface Science and Catalysis, 2004, 154, 924-930.	1.5	5
264	Transportation of molecules with a scanning tunneling microscope. Applied Physics Letters, 2006, 89, 103114.	1.5	5
265	Hidden crystalline components in mesoporous silicate. Journal of Materials Chemistry, 2012, 22, 23141.	6.7	5
266	Growth mechanisms of Ag and Cu nanodendrites via Galvanic replacement reactions. Progress in Natural Science: Materials International, 2021, 31, 141-151.	1.8	5
267	NIR-assisted orchid virus therapy using urchin bimetallic nanomaterials in phalaenopsis. Advances in Natural Sciences: Nanoscience and Nanotechnology, 2013, 4, 045006.	0.7	4
268	Naturally Occurring and Biomimetic Synthesized Calcite Spherulites. Crystal Growth and Design, 2020, 20, 3537-3545.	1.4	4
269	Site-Directed Surface Derivatization of MCM-41: Use of High-Resolution Transmission Electron Microscopy and Molecular Recognition for Determining the Position of Functionality within Mesoporous Materials. , 1998, 37, 2719.		4
270	Reversed crystal growth of metal organic framework MIL-68(In). CrystEngComm, 2021, 23, 7658-7662.	1.3	4

#	Article	IF	CITATIONS
271	Imaging Oxygen Vacancies in Superconducting YBa2Cu3O7–Î′ by High Resolution Electron Microscopy. Angewandte Chemie International Edition in English, 1987, 26, 1048-1050.	4.4	3
272	HRTEM surface characterization of nanoscale solid-state materials. Surface and Interface Analysis, 2001, 32, 236-239.	0.8	3
273	Mesoporous silicas of hierarchical structure by hydrothermal surfactant-templating under mild alkali conditions. Studies in Surface Science and Catalysis, 2002, 141, 133-140.	1.5	3
274	Study of the initial adsorption state of tetracene on. Journal of Physics Condensed Matter, 2007, 19, 296202.	0.7	3
275	Dual-Step Reduction of Copper and Formation Mechanism of Cu Pseudo-Icosahedral Microcrystals. Crystal Growth and Design, 2022, 22, 2611-2619.	1.4	3
276	A New Family of Photoactive Catalysts Based Upon Bismuth Oxide. Materials Research Society Symposia Proceedings, 1987, 111, 295.	0.1	2
277	Ordering of lanthanum(3+) ions in the bismuth(3+) sublattice of layered oxychloride catalysts. Chemistry of Materials, 1990, 2, 215-216.	3.2	2
278	Mesoporous crystals of metal oxides and their properties. Studies in Surface Science and Catalysis, 2007, 165, 335-338.	1.5	2
279	Electron microscopic studies of growth of nanoscale catalysts and soot particles in a candle flame. Applied Petrochemical Research, 2012, 2, 15-21.	1.3	2
280	Facile Synthesis of (110)â€Planeâ€Exposed Au Microflowers as High Sensitive Hydrogen Peroxide Sensors. European Journal of Inorganic Chemistry, 2015, 2015, 2528-2533.	1.0	2
281	Incommensurate–Commensurate Transition in the Geometric Ferroelectric LaTaO ₄ . Advanced Functional Materials, 2020, 30, 2004667.	7.8	2
282	Electron microscopic investigation of mesoporous SBA-2. Studies in Surface Science and Catalysis, 2002, 141, 379-386.	1.5	1
283	Studies on the perovskite-based La4Srnâ^'4TinO3n+2. Materials Research Society Symposia Proceedings, 2003, 801, 204.	0.1	1
284	Cobalt Diselenide Nanorods Grafted on Graphitic Carbon Nitride: A Synergistic Catalyst for Oxygen Reactions in Rechargeable Liâ^'O2 Batteries. ChemElectroChem, 2018, 5, 5-5.	1.7	1
285	Controlled Synthesis of Carbon-Encapsulated Co Nanoparticles by CVD. , 2001, 7, 248.		1
286	Growth mechanism and microstructures of Cu ₂ O/PVP spherulites. RSC Advances, 2022, 12, 20022-20028.	1.7	1
287	Zeolite GdNaY Nanoparticles with Very High Relaxivity for Application as Contrast Agents in Magnetic Resonance Imaging ChemInform, 2003, 34, no.	0.1	0
288	Direct and post- hydrothermal treatments in ammoniated solution for the morphogenesis of mesoporous silica nanotubes. Studies in Surface Science and Catalysis, 2003, 146, 181-184.	1.5	0

#	Article	IF	CITATIONS
289	Recyclable Polyurea-Microencapsulated Pd(0) Nanoparticles: An Efficient Catalyst for Hydrogenolysis of Epoxides ChemInform, 2004, 35, no.	0.1	0
290	Synthesis and Structure of Bimetallic Nickel Molybdenum Phosphide Solid Solutions ChemInform, 2004, 35, no.	0.1	0
291	TNU-7: A Large-Pore Gallosilicate Zeolite Constructed of Strictly Alternating MOR and MAZ Layers ChemInform, 2005, 36, no.	0.1	0
292	Tuned Light Emission from Nanoparticles of Cadmium Chalcogenides and Nanostructures in Indium Nitride. Synthesis and Reactivity in Inorganic, Metal Organic, and Nano Metal Chemistry, 2007, 37, 309-313.	0.6	0
293	Transmission Electron Microscopy. , 0, , 443-485.		0
294	Ten years of electron microscopy of nanomaterials in St. Andrews. International Journal of Nanotechnology, 2012, 9, 69.	0.1	0
295	Nanoporous nanocrystalline monoclinic zirconia for luminescent oxygen sensors. Proceedings of SPIE, 2015, , .	0.8	0
296	Formation mechanism of Mn _{<i>x</i>} Co _{3â~'<i>x</i>} O ₄ yolk–shell structures. RSC Advances, 2021, 11, 29108-29114.	1.7	0
297	Exploration of New Porous Solids in the Search for Adsorbents and Catalysts. , 2007, , 123-137.		0
298	SYNTHESIS OF ZEOLITE ZSM-5 COMPOSITES WITH A SINGLE TEMPLATE. , 2008, , .		0
299	Disruption of extended defects in solid oxide fuel cell anodes for methane oxidation. , 2010, , 251-254.		0